S. HARABASZ
for the HADES Collaboration
Institut für Kernphysik, Technische Universität Darmstadt/GSI
(9, Schlossgartenstr., 64289 Darmstadt, Germany; e-mail: s.harabasz@gsi.de)

UDC 539

EXPLORING BARYON RICH MATTER WITH HEAVY-ION COLLISIONS

Collisions of heavy nuclei at (ultra-)relativistic energies provide a fascinating opportunity to re-create various forms of matter in the laboratory. For a short extent of time (10^{-22} s), matter under extreme conditions of temperature and density can exist. In dedicated experiments, one explores the microscopic structure of strongly interacting matter and its phase diagram. In heavy-ion reactions at SIS18 collision energies, matter is substantially compressed (2–3 times ground-state density), while moderate temperatures are reached ($T < 70$ MeV). The conditions closely resemble those that prevail, e.g., in neutron star mergers. Matter under such conditions is currently being studied at the High Acceptance DiElecton Spectrometer (HADES). Important topics of the research program are the mechanisms of strangeness production, the emissivity of matter, and the role of baryonic resonances herein. In this contribution, we will focus on the important experimental results obtained by HADES in Au + Au collisions at 2.4 GeV center-of-mass energy. We will also present perspectives for future experiments with HADES and CBM at SIS100, where higher beam energies and intensities will allow for the studies of the first-order deconfinement phase transition and its critical endpoint.

K e y w o r d s: heavy-ion collisions, HADES, vector meson dominance, dileptons, strangeness.

1. Introduction

When two heavy ions collide at relativistic energies, they form matter of high temperature (10^{12} K) and density ($< 3\rho_0$). The exact values and, thus, the detailed properties of the matter depend on the kinetic energy of the collision. While, at $\sqrt{s_{\rm NN}}$ of the order of hundreds GeV or of TeV, the properties of the matter resemble that, which prevailed in the Universe shortly after the Big Bang, with energies of few GeVs, thermodynamic conditions are similar to neutron star mergers (see, e.g., [1]). The scan of beam energies in between probes the phase diagram of a strongly interacting matter (search for a first-order phase transition and a critical point). Through the relation between a phase structure and symmetry patterns, it sheds light on the problems of quark confinement and hadron mass generation.

In this paper, we will present the results on the production of strange hadrons and dileptons in Au + Au collisions at $\sqrt{s_{\rm NN}} = 2.4$ GeV obtained by HADES. We will put them in context of earlier results on the dilepton production in nucleon-nucleon (pp and np) reactions at the same collision energy (per nucleon).

2. Experimental Setup

HADES is a fixed-target setup installed at SIS18 (*Schwerionen-Synchrotron* with rigidity 18 Tm) accelerator in Darmstadt, Germany [2]. It possess a six-fold symmetry defined by identical sectors covering nearly 60 degrees of the azimuthal angle each. Within the sectors, the particle tracking and momentum reconstruction are provided by the toroidal magnetic field generated by compact superconducting coils located between sectors and by four Multiwire Drift Chambers (MDCs): two upstream and two downstream to the magnetic field region. The tracking resolution for lepton pair invariant masses close to vector meson poles is of the order of few % ($\delta M = 15$ MeV/c^2 at $M = 780$ MeV/c^2).

Behind the tracking system, time-of-flight detectors are located. Above the polar angle of about 45 degree, a wall of plastic scintillator bars is mounted, at lower polar angles, Resistive Plate Chambers

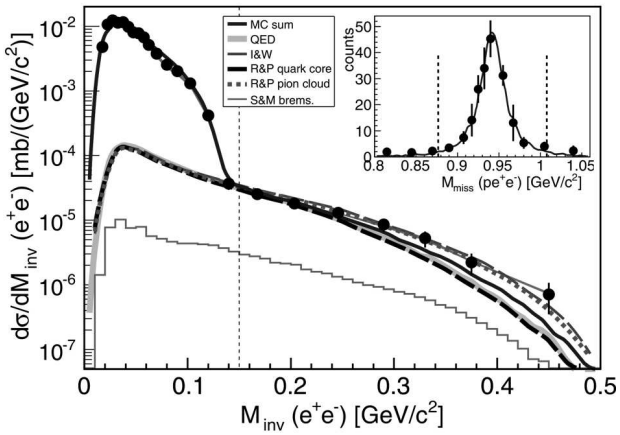

Fig. 1. e^+e^- invariant mass within the HADES acceptance. Experimental data (black dots) are corrected for the detection and reconstruction inefficiencies. Curves represent models, as discussed in the text

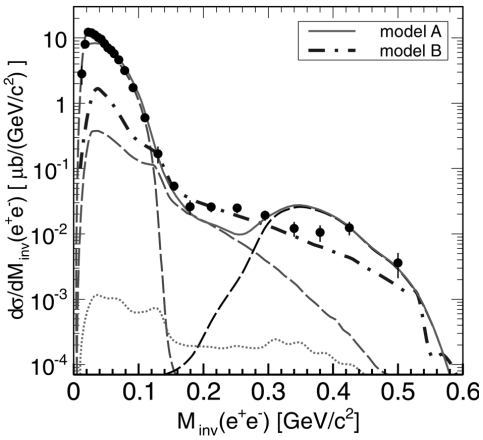

Fig. 2. Dielectron differential cross section as a function of the invariant mass of e^+e^- within the HADES acceptance. The data (black dots) are corrected for the detection and reconstruction inefficiencies. The simulated cocktail (curves) of the π^0 (dashed violet), η (dotted magenta), Δ (dashed red) Dalitz decays, ρ from the $\Delta - \Delta$ interaction process (dashed black) according to the model [4] and the sum (contributions from π^0, η, Δ and ρ – solid green curve) are displayed – model A. The dotted-dashed blue curve shows the bremsstrahlung contribution from [6] – model B

(RPCs) are installed, which have granularity necessary for high-multiplicity Au + Au events. After the proper calibration, the intrinsic time resolution of the scintillator wall is 150 ps and that of RPC – below 70 ps. Behind the RPC, an electromagnetic Pre-Shower detector is located, which contributes to the lepton identification. In each sector, it consists of two lead converter plates sandwiched between three wire chambers in the streamer mode.

The main role in the lepton identification task is played by a Ring Imaging Cherenkov (RICH) detector. It is placed in front of the tracking system in the field-free region. It consists of a single chamber filled with C_4F_{10} radiator gas, closed by a spherical mirror in the forward direction and separated from the photon detector by a CaF_2 window in the backward direction. The photon detector is an MWPC with aa planar CsI photocathode divided into pads in such a way that Cherenkov light emitted in the radiator and reflected from the mirror forms rings on the cathode plane, whose radii in terms of the number of pads are independent of the location. For C_4F_{10}, the threshold Lorentz γ for Cherenkov emission is 18. This translates to the threshold momenta for electrons of 0.01 GeV/c, for muons of 1.9 GeV/c, and for pions of 2.4 GeV/c. With the energy available for the particle production at $\sqrt{s_{\rm NN}} = 2.4$ GeV collisions, the very fact of the Cherenkov radiation emission discriminates between electrons and other particles.

The spectrometer is also equipped with a CVD (chemical vapor deposition) diamond t_0 detector placed in front of and a VETO detector behind the target. About 7 m downstream the target, a Forward Wall hodoscope is located. The Au target was split into 15 segments, each 20 μm thick, in order to reduce the conversion probability of real photons in the target.

3. Dileptons in $p + p$ and $n + p$

Collisions of single hadrons (nucleon-nucleon and pion-nucleon) allow for determining various resonance properties in elementary collisions, in particular the electromagnetic transition form factors. Via the Dalitz decays, they can be studied in the kinematic region $0 < q^2 < 4m_p^2$ (m_p is the proton mass), which is not accessible in annihilation experiments.

The analysis of the exclusive channel $pp \to ppe^+e^-$ with a kinetic energy of 1.25 GeV of the beam allowed HADES to measure, for the first time, the branching ratio of the decay $\Delta \to pe^+e^-$. It equals $(4.19 \pm 0.62 \pm 0.34) \times 10^{-5}$, where the former uncertainty is systematic, including the model dependence, and the latter is statistical [12].

Figure 1 shows the invariant mass distribution of dileptons from $p + p$ collisions after the cut on the

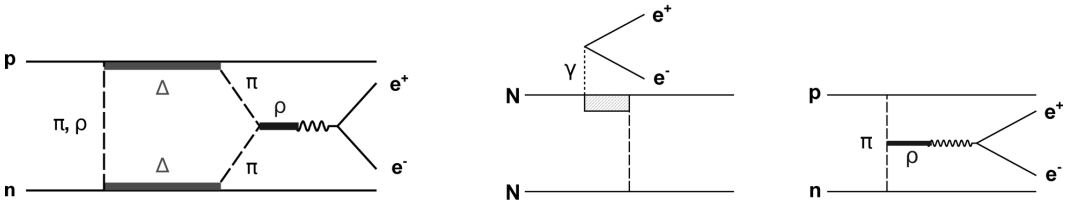

Fig. 3. Left: one of the diagrams contributing to the $\Delta - \Delta$ interaction in model A [4] of Fig. 2. Middle and right: diagrams contributing to the coherent sum in the bremsstrahlung description of [6]

proton missing mass indicated in the inset, compared to different models of the Δ form factor. The blue curve represents the sum of the following contributions: π^0 Dalitz decay, Δ Dalitz decay according to [5], and bremsstrahlung according to [6]. The cyan curve is the Δ Dalitz contribution in a description with a point-like $\gamma^* NR$ coupling ("QED-model") [7, 8], fixed from reactions with $q^2 = 0$. The two-component Iachello–Wan model [9–11], depicted with the dashed dark green curve, has the largest contribution. It parametrizes the electromagnetic interaction by a direct coupling and a coupling via a vector meson with dressed ρ propagator. The constituent quark model by Ramalho and Peña [5] describes the dominant G_M^* form factor with two contributions: quark core (quark-diquark S-wave) and pion cloud (photon directly coupling to a pion or to an intermediate baryon state). The two components are shown after scaling each of them up to the same yield as in the full model: quark core (dashed black curve) and pion cloud (dashed red curve). All model contributions are supplemented with the bremsstrahlung (shown also separately as a green histogram).

It should be noted that the quark-core contribution of the Ramalho–Peña model nearly coincides with the "QED-model," and both are not sufficient to describe the experimental data. An additional coupling in terms of the pion could/intermediate ρ meson seems to be necessary.

The role of a ρ meson is also highlighted by the np measurement [13]. It was performed by colliding a deuterium beam with a kinetic energy $1.25A$ GeV and selecting events with a quasifree neutron through the proton detection in a forward hodoscope. The cross-section distribution for the e^+e^- production over the pair invariant mass is shown in Fig. 2. It is compared to two model calculations. Model A includes hadronic sources, as well as $\Delta - \Delta$ interaction, as shown in the left-most panel of Fig. 3 (other

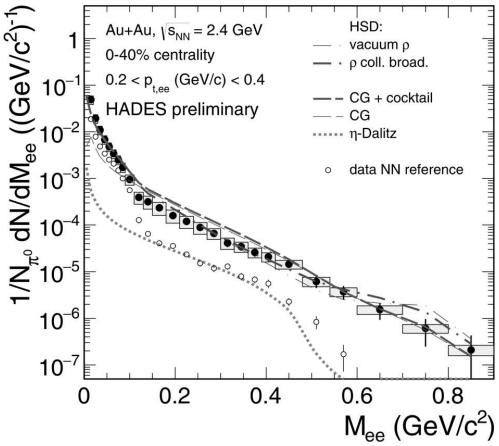

Fig. 4. Invariant mass distribution of e^+e^- from Au + Au collisions at $\sqrt{s_{\rm NN}} = 2.4$ GeV. It was corrected for the detection efficiency, extrapolated to 4π and the zero single-lepton momentum and normalized to the π^0 multiplicity. Similarly, the corrected normalized distribution from the reference pp and np reactions is shown as well. Curves represent theoretical model calculations: [18] (HSD), [16] (CG). The latter is accompanied by a cocktail of hadronic sources at the freeze-out (these sources are already included in the HSD calculation). The largest contribution to the cocktail above the π^0 mass, $\eta \to \gamma e^+ e^-$, is shown separately

diagrams permuting incoming and outgoing propagators are also included). Model B contains only bremsstrahlung, described in [6] in terms of diagrams like shown in the middle and the right panel of Fig. 3 (with appropriate permutations). Model A underestimates the cross-section in the invariant mass region of 0.15–0.3 GeV/c^2. The bremsstrahlung contribution goes though the experimental points here. A full model adding all the contributions, perhaps coherently, would be needed. But the results indicate that the interaction via the pion exchange or annihilation of virtual pions with the subsequent emission of a ρ meson plays an important role in hadronic interactions.

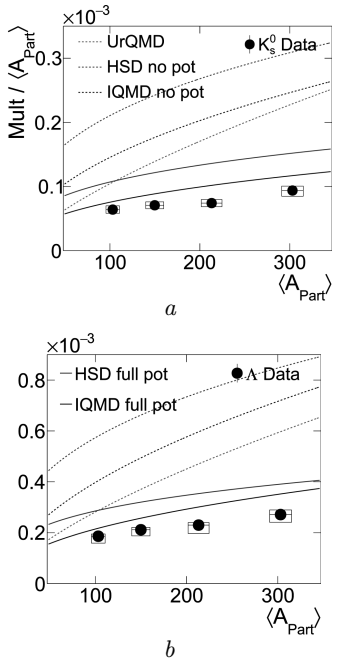

Fig. 5. Multiplicities per mean number of participants Mult/$\langle A_{\rm part}\rangle$, as a function of $\langle A_{\rm part}\rangle$ for K^0_s (a) and Λ (b) compared to various transport model calculations

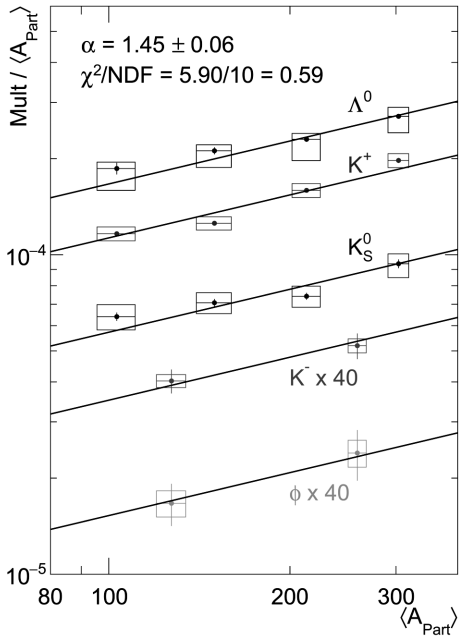

Fig. 6. Multiplicities per mean number of participants Mult/$\langle A_{\rm part}\rangle$ as a function of $\langle A_{\rm part}\rangle$. All hadron yields are fitted simultaneously with a function of the form Mult $\propto \langle A_{\rm part}\rangle^{\alpha}$ with the result: $\alpha = 1.45 \pm 0.06$

4. Dileptons in Heavy-Ion Collisions

In heavy-ion collisions, the dileptons are not scattered or reabsorbed through the strong interaction with hadronic matter. Thus, they can probe the interior and early stages of the evolution of a hot dense fireball. Their multiplicity will be ever-increasing with fireball's lifetime, and the spectra will take exponential shape with the slope reflecting the effective temperature of the system, which should be higher than the freeze-out temperature extracted from the spectra of hadrons that decouple in the late stage of the collision.

Figure 4 shows the invariant mass distribution of the radiation of dileptons at $\sqrt{s_{\rm NN}} = 2.4$ GeV, for a pair transverse momentum $p_{\rm t,ee}$ range of 0.2–0.4 GeV/c. It is compared to the spectrum from pp and np reactions which represents, after a proper normalization, first-chance collisions between nucleons participating in a heavy-ion reaction ("NN reference"). The excess amounts to the factor of 8–10 in the mass range above the π^0 mass, see also [14]. By comparing to the ρ spectra from the transport model HSD [18], where a ρ meson is treated as free or subject to the collisional broadening, one can note that the resonant structure completely disappears ("melts") in the experiment. This feature is captured by different implementations of the relatively novel approach of coarse-graining (CG) [15–17], where the explicit assumption of local thermal equilibrium is made. It is used to calculate the temperature and density of small space-time cells of a fireball (with transport models as the input). These are used to calculate the thermal dilepton emission using a vector meson (ρ dominating) spectral function. Coarse-graining approaches also make use of the vector meson dominance (VMD) assumption, according to which all the dilepton emission proceeds through an intermediate vector meson. Their validity is strengthened by the aforementioned findings in NN collisions.

At lower values of the invariant mass, all the models leave room for an improvement, and the higher statistics data with a higher signal-to-background ratio (main source of the systematic uncertainty) would be of great importance.

5. Strangeness Production in Heavy-Ion Collisions

Collision energies at SIS18 are below the strangeness production threshold in NN collisions. Therefore, the

multiplicities and spectra of strange particles in heavy-ion reactions are sensitive to the mechanisms of energy accumulation and possibly to the equation of state of the strongly interacting matter.

Figure 5 shows the multiplicities of K^0_s and Λ as functions of the mean number of nucleons participating in the collision, $\langle A_{\rm part}\rangle$ in Au + Au at $\sqrt{s_{\rm NN}} =$ = 2.4 GeV [19]. It is compared to a number of transport models: UrQMD [21], IQMD [22], and HSD [23]. For HSD and IQMD, two versions of a simulation were done: with a repulsive K-N potential of 40 MeV at the nuclear ground state density ρ_0, which increases linearly with the density, and without such a potential. Turning on the potential brings the theory predictions closer to the experimental data, both in terms of the multiplicity values and of the α exponent in the power law Mult $\propto \langle A_{\rm part}\rangle^{\alpha}$. The large spread between the models themselves would result in the value of the potential strongly model-dependent.

The $\langle A_{\rm part}\rangle$ dependence of the multiplicities of all strange particles reconstructed in HADES (K^+, K^-, ϕ [20], K^0_s, and Λ [19]) is displayed in Fig. 6. Data for all the particles can be described by the power law with the same exponent. This does not reflect the hierarchy in NN thresholds for different strange particles and is not expected, if the energy for their production is accumulated in a sequence of isolated nucleon-nucleon collisions. Instead, we suggested in [19] that the total amount of strange quarks in a collision is produced according to the system size determined by the number of participating nucleons. Their distribution between hadrons is fixed at the freeze-out.

6. Conclusions

HADES provides the high-statistics and high-precision data on the particle production in Au + Au collisions at the relatively low energy $\sqrt{s_{\rm NN}} = 2.4$ GeV. In this contribution, a selection of results was presented, which suggests that the hot dense fireball created in such collisions is a much stronger correlated system, than it was assumed up to now. These correlations might allow for a faster thermalization of the system, a statistical redistribution of strange quarks among hadrons, and the melting of a ρ meson. These cannot be exactly reproduced by the conventional hadronic transport models. It remains to be rigorously studied on the ground of theory and phenomenology, if the correlations can be attributed to a "pion cloud" of hadron (or another formalism), whose effect is clearly visible in NN collisions. If the density-dependent repulsive effective K-N potential can be regarded as a proxy for the nontrivial hadron structure, then the improvement in the description of the Mult($\langle A_{\rm part}\rangle$) dependence for K^0_s and Λ could also be a manifestation of this structure.

7. Outlook

On the experimental side, the understanding of the effects observed in heavy-ion collisions requires more data with various colliding systems and beam energies. To this end, HADES measured Ag + Ag collisions at $\sqrt{s_{\rm NN}} = 2.4$ GeV and $\sqrt{s_{\rm NN}} = 2.55$ GeV in March 2019. The statistics of events at the former energy is slightly lower as in Au + Au at $\sqrt{s_{\rm NN}} =$ = 2.4 GeV, while it is a few times higher at the latter energy. Moreover, in Ag + Ag, the combinatorial background in the reconstruction of unstable particles is expected to be smaller, than in Au + Au. Therefore, it will very likely that the main physical results of Au + Au can be extended to Ag + Ag at both collision energies.

In the future FAIR (Facility for Antiproton and Ion Research) in Darmstadt, currently under the construction, the CBM (Compressed Baryonic Matter) experiment will collide heavy ions at energies of $\sqrt{s_{\rm NN}}$ from roughly 3 to 6 GeV. This will fill the gap in energy between the existing data of HADES and STAR at Relativistic Heavy-Ion Collider in Brookhaven. It will collect data with an unprecedented interaction rate of 10 MHz (0.5 MHz from day 1), which will allow for the studies of rare and penetrating probes, in particular, dileptons and multistrange particles and for the search of the critical point of the deconfinement phase transition. HADES at SIS100 will focus mainly on the e^+e^- and strangeness production in pp and pA collisions.

We gratefully acknowledge the support by the grants SIP JUC Cracow (Poland), 2013/10/M/ST2/00042; TU Darmstadt (Germany), VH-NG-823; GU Frankfurt, (Germany), BMBF:05P15RFFCA, HIC for FAIR, ExtreMe Matter Institute EMMI; TU MГjnchen, Garching (Germany), MLL MГjnchen, DFG EClust 153, DFG FAB898/2-1, BmBF 05P15WOFCA; JLU Giessen (Germany),

BMBF:05P12RGGHM; IPN, IN2P3/CNRS (France); NPI CAS Rez (Czech Republic), GACR 13-06759S, MSMT LM2015049.

1. M. Hanauske *et al.* Neutron star mergers: Probing the EoS of hot, dense matter by gravitational waves. *Particles* **2**, 44 (2019).
2. G. Agakichiev *et al.* (HADES). The high-acceptance dielectron spectrometer HADES. *Eur. Phys. J. A* **41**, 243 (2009).
3. G. Ramalho, M.T. Peña, J. Weil, H. van Hees, U. Mosel. Role of the pion electromagnetic form factor in the $\Delta(1232) \to \gamma^* N$ timelike transition. *Phys. Rev. D* **93**, 033004 (2016).
4. M. Bashkanov, H. Clement. On a Possible Explanation of the DLS Puzzle. *Eur. Phys. J. A* **50**, 107 (2014).
5. G. Ramalho, M.T. Peña, J. Weil, H. van Hees, U. Mosel. The high-acceptance dielectron spectrometer HADES. *Phys. Rev. D* **93**, 033004 (2016).
6. R. Shyam, U. Mosel. Dilepton production in proton-proton and quasi-free proton-neutron reactions at 1.25 GeV. *Phys. Rev. C* **82**, 062201 (2010).
7. M. Zétényi, Gy. Wolf. Dilepton decays of baryon resonances. *Heavy Ion Phys.* **17**, 27 (2003).
8. F. Dohrmann *et al.* A versatile method for simulating $\mathrm{pp} \to \mathrm{pp}\ \mathrm{e^+e^-}$ and $\mathrm{dp} \to \mathrm{pn}\ \mathrm{e^+e^-}$ p(spec) reactions. *Eur. Phys. J. A* **45**, 401 (2010).
9. F. Iachello and Q. Wan. Structure of the nucleon from electromagnetic timelike form factors. *Phys. Rev. C* **69**, 055204 (2004).
10. Q. Wan, F. Iachello. A unified description of baryon electromagnetic form factors. *Int. J. Mod. Phys. A* **20**, 1846 (2005).
11. Q. Wan, PhD Thesis. A Unified Approach to Baryon Electromagnetic Form Factors (Yale University, New Haven, 2007).
12. J. Adamczewski-Musch *et al.* (HADES Collaboration). $\Delta(1232)$ Dalitz decay in proton-proton collisions at $T = 1.25$ GeV measured with HADES at GSI. *Phys. Rev. C* **95**, 065205 (2017).
13. J. Adamczewski-Musch *et al.* (HADES Collaboration). entrality determination of Au + Au collisions at 1.23 A GeV with HADES. *Eur. Phys. J. A* **53**, 149 (2017).
14. J. Adamczewski-Musch *et al.* (HADES Collaboration). Probing dense baryon-rich matter with virtual photons. *Nature Physics.* https://doi.org/10.1038/s41567-019-0583-8.
15. S. Endres *et al.*. Dilepton production and reaction dynamics in heavy-ion collisions at SIS energies from coarse-grained transport simulations. *Phys. Rev. C* **92**, 014911 (2015).
16. T. Galatyuk *et al.* Thermal dileptons from coarse-grained transport as fireball probes at SIS energies. *Eur. Phys. J. A* **52**, 131 (2016).
17. J. Staudenmaier *et al.* Dilepton production and resonance properties within a new hadronic transport approach in the context of the GSI-HADES experimental data. *Phys. Rev. C* **98**, 054908 (2018).
18. E. L. Bratkovskaya *et al.* System size and energy dependence of dilepton production in heavy-ion collisions at 1–2 GeV/nucleon energies. *Phys. Rev. C* **87**, 064907 (2013).
19. J. Adamczewski-Musch *et al.* (HADES Collaboration). Sub-threshold production of K^s_0 mesons and Λ hyperons in Au + Au collisions at $\sqrt{s_{NN}} = 2.4$ GeV. *Phys. Lett. B* **793**, 457 (2019).
20. J. Adamczewski-Musch *et al.* (HADES Collaboration). Deep sub-threshold ϕ production in Au + Au collisions. *Phys. Lett. B* **778**, 403 (2018).
21. S.A. Bass *et al.* Microscopic models for ultrarelativistic heavy ion collisions. *Prog. Part. Nucl. Phys.* **41**, 225 (1998).
22. C. Hartnack. *et al.* Modeling the many body dynamics of heavy ion collisions: Present status and future perspective. *Eur. Phys. J. A* **1**, 151 (1998).
23. W. Cassing, E.L. Bratkovskaya. Hadronic and electromagnetic probes of hot and dense nuclear matter. *Phys. Rept.* **308**, 65 (1999).

Received 08.07.19

С. Гарабаш

ДОСЛІДЖЕННЯ БАРІОННОЇ
МАТЕРІЇ В ЗІТКНЕННЯХ ВАЖКИХ ІОНІВ

Р е з ю м е

Зіткнення важких іонів при (ультра-)релятивістських енергіях дають чудову можливість для створення різних форм речовини в лабораторії. Короткий час (10^{-22} сек) може існувати речовина з екстремальними температурою та щільністю. В спеціальних експериментах вивчається мікроскопічна структура сильновзаємодіючої речовини і її фазова діаграма. В реакціях з важкими іонами при енергіях SIS18 речовина значно стискається (в 2–3 рази порівняно зі щільністю основного стану) при помірних температурах ($T < 70$ МеВ). Ці умови нагадують, наприклад, стан колапсу нейтронних зірок. Речовина при таких умовах власне вивчається на HADES (High Acceptance DIElectron Spectrometer). Важливими в рамках цієї програми є дослідження механізму продукування дивності, випромінювання матерії та роль в цьому баріонних резонансів. В даній роботі ми звертаємо увагу на важливі експериментальні результати, отримані на HADES у зіткненнях Au+Au при енергії в системі центра мас 2,4 ГеВ. Ми також представимо перспективи майбутніх експериментів з HADES та CBM при SIS100, де більш високі енергії та інтенсивності дозволять вивчати фазовий перехід першого роду деконфайнменту та відповідну йому критичну точку.